

KEUNHYUK RYU¹, MYUNGSUK KIM¹, JAESEOK ROH¹, KUN-JAE LEE^{1*}

DISSOLUTION BEHAVIOR OF METAL IMPURITIES AND IMPROVEMENT OF RECLAIMED SEMICONDUCTOR WAFER CLEANING BY ADDITION OF CHELATING AGENT

As a wafer cleaning process, RCA (Radio Corporation of America) cleaning is mainly used. However, RCA cleaning has problems such as instability of bath life, re-adsorption of impurities and high-temperature cleaning. Herein, we tried to improve the purity of silicon wafers by using a chelating agent (oxalic acid) to solve these problems. Compounds produced by the reaction between the cleaning solution and each metal powder were identified by referring to the pourbaix diagram. All metals exhibited a particle size distribution of 10 μm or more before reaction, but a particle size distribution of 500 nm or less after reaction. In addition, it was confirmed that the metals before and after the reaction showed different absorbances. As a result of elemental analysis on the surface of the reclaimed silicon wafer cleaned through such a cleaning solution, it was confirmed that no secondary phase was detected other than Si.

Keywords: Reclaimed silicon wafer, Wafer cleaning, Metal impurity, Metal complex, Chelating agent

1. Introduction

Silicon wafers are basic material widely used in semiconductor device manufacturing due to their unique electronic and mechanical properties [1]. Silicon wafer uses include reclaimed wafers used for process monitoring, which can be manufactured by reprocessing waste wafers [2]. However, impurities remaining in the waste wafer and impurities generated in the process of manufacturing the reclaimed wafer negatively affect the silicon wafer properties [3-5]. Therefore, cleaning technology to remove contaminants from the silicon wafer surface is essential [6].

RCA cleaning is mainly used as a wafer cleaning process [7,8]. However, RCA cleaning has problems such as re-adsorption of metal impurities, etching of wafer surface due to strong acid, shortening of bath life and high temperature required [9].

This problem of conventional RCA cleaning can be solved by adding chelating agents to the cleaning solution. By adding chelating agents, H_2O_2 decomposition can be prevented, improving bath life stability and preventing wafer surface roughness improvement. In addition, re-adsorption of metal impurities may be prevented through stable bonding between chelating agent and metal impurities. Therefore, in this study, we tried to solve

problems of RCA cleaning and improve the purity of the silicon wafer through chelating agent.

2. Experimental

2.1. Metal dissolution and wafer cleaning by chelating agent

Fe (99%, Aldrich), Zn (99%, DAEJUNG), Al (99.5%, DAEJUNG) and Cu (99.85%, KANTO CHEMICAL CO., INC.), Cr (99%, DAEJUNG), Ni (99%, DAEJUNG) which are common metal impurities present on wafer surface, were charged into a 70 mL vial containing 50 mL cleaning solution each of 0.018 g and reacted in the ultrasonicator for 12 hours. The coolant of the ultrasonicator was continuously circulated, and experiment was conducted by maintaining about 25°C. The experiment was conducted by measuring ionic conductivity at 3 hour intervals. The cleaning solution composition was prepared by loading 0.33 mol of oxalic acid (98.5%, DAEJUNG), 400 mL of H_2O_2 (30%, DAEJUNG) and 50 mL of NH_4OH (25.0~28.0%, DAEJUNG) with reference to the pourbaix diagram. The waste wafer was sampled at $1 \times 1 \text{ cm}^2$, and cleaned for 10 minutes by immersing in a cleaning solution newly prepared with the same composition.

¹ DANKOOK UNIVERSITY, DEPARTMENT OF ENERGY ENGINEERING, CHEONAN 31116, REPUBLIC OF KOREA

* Corresponding author: kjlee@dankook.ac.kr



2.2. Characterization

The dissolution behavior of each metal over time was analyzed through a conductivity meter (SevenExcellence, METTLER TOLEDO). Particle size change and absorbance were analyzed before and after reaction by dynamic light scattering (DLS, Otsuka Electronics, NanoPlus-3) and ultraviolet-visible spectroscopy (UV-1800, SHIMADZU). All analysis of particle size change before and after the reaction was performed using D.I water as a solvent. The pourbaix diagram was calculated by entering the cleaning solution composition in software (Hydra/Medusa). Before and after cleaning, the wafer surface shape analysis was performed through field emission scanning electron microscope (FE-SEM, ZEISS, Gemini). The waste wafer surface elemental analysis was performed before cleaning through energy dispersive X-ray microanalysis (EDS, EDAX Pegasus 4040, EDAX), and the same sample was cleaned and elemental analysis was again performed to confirm the cleaning rate of the cleaning solution.

3. Results and discussion

Fig. 1 shows pourbaix diagram for the reaction of each metal element by the cleaning solution. All metals react with the

cleaning solution from about pH 1 to pH 7 to form compounds. The reactivity between the chelating agent and metal impurities is higher under the high pH condition than under the low pH condition. This is related to competition between metal and hydronium ions for the same active site. As the pH increases, the hydronium ion decreases, so the reaction between the metal ion and the chelating agent increases [10]. In addition, since there is no surface charge under low pH conditions, there is a problem that metal impurities are re-adsorbed [9]. Therefore, the pH of the cleaning solution was set to pH 7, which is the highest pH condition among the pH ranges in which the cleaning solution and metal react to form a coordination compound. According to pourbaix diagram, Fe, Zn, Al, Cu, Cr and Ni react with the cleaning solution to form coordination compounds such as $Fe(ox)_3^{3-}$, $Zn(NH_3)_4^{2+}$, $Al(ox)_3^{3-}$, $Cu(NH_3)_2^+$, $Cr(NH_3)_5OH^{2+}$ and $Ni(NH_3)_6^{2+}$ respectively.

Fig. 2 shows particle size and UV data before and after the reaction of metal powders. As shown in Fig. 2(a), the particle sizes of Fe, Zn and Al before the reaction were 12 μm , 16 μm and 10 μm , respectively, but after the reaction, the particle size distribution was about 270 nm. In addition, as shown in Fig. 2(b), since the metal before the reaction, the metal after the reaction, and the cleaning solution all showed different absorbances, it is expected that metal dissolution occurred by the following reaction equations [11-13].

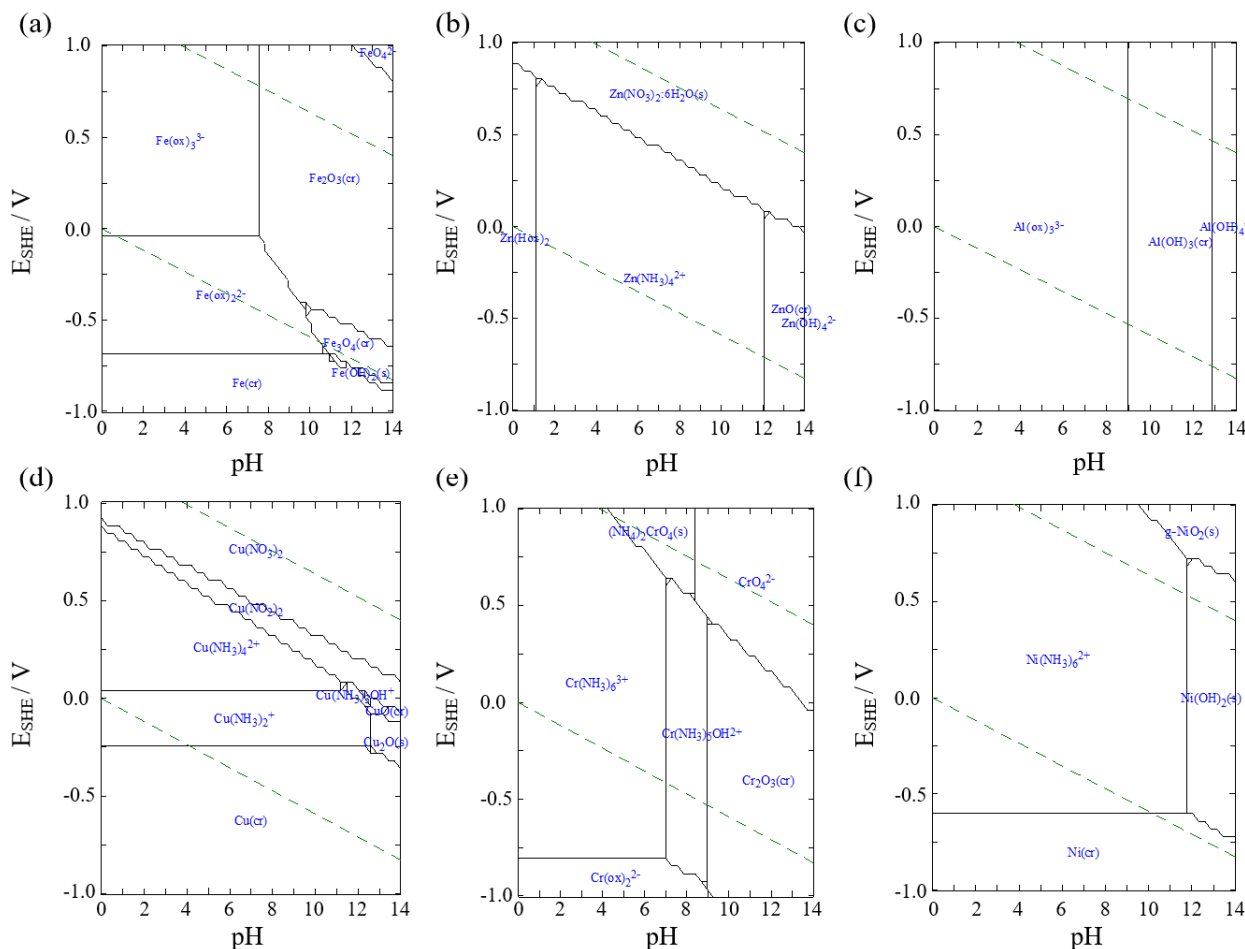
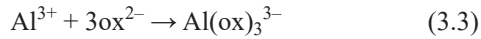
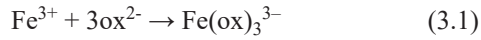


Fig. 1. Pourbaix diagram of metal in cleaning solution containing oxalic acid (a) Fe, (b) Zn, (c) Al, (d) Cu, (e) Cr, (f) Ni



As shown in Fig. 2(c), the particle sizes of Cu, Cr and Ni before the reaction were 16 μm , 18 μm and 29 μm , respectively, but after the reaction, the particle size distribution was about 475 nm. In addition, as shown in Fig. 2(d), since the metal before reaction, the metal after reaction, and the cleaning solution all showed different absorbances, it is expected that metal dissolution occurred by the following reaction equations [14-17].

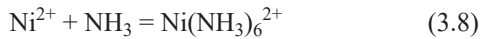
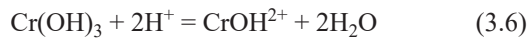
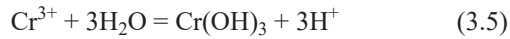


Fig. 3 shows the dissolution behavior of metal powder over time. Fig. 3(a) shows the change in ionic conductivity of FeZnAl over time. Ionic conductivity of FeZnAl showed a rapid increase after 3 hours of reaction and showed a tendency to rise gently over time. This is expected to be the effect of saturation.

In addition, since the ionic conductivity of FeZnAl showed a tendency to increase after 3 hours of reaction than before reaction, it is expected that H_2O_2 decomposition was prevented by the chelating agent having strong corrosion resistance against oxidative decomposition. Fig. 3(b) shows the change in ionic conductivity of CuCrNi over time. Ionic conductivity of CuCrNi showed a relatively irregular tendency rather than increasing by the time. This is expected to be influenced by the additional dissolution of Cr and Ni, which has slow reaction rate. In addition, since the ionic conductivity slightly decreased by about 3.82% after the reaction for 3 hours compared to before the reaction, it is expected that H_2O_2 decomposition was prevented by the chelating agent. As shown in Table 1, the metal impurities detected as a result of elemental analysis on the waste wafer surface before cleaning were identified as Al, Fe and Zn etc.

TABLE 1

Type and content of impurities detected on the waste wafer surface before cleaning

Atom %										
C	O	F	Na	Mg	Al	Si	S	Ca	Fe	Zn
2.93	19.48	27.26	10.60	0.93	0.03	36.77	0.65	0.53	0.13	0.71

Fig. 4 shows the surface shape and elemental analysis results of the wafer cleaned for 10 minutes in the cleaning solution. As can be seen in Fig. 4(a), it was confirmed that a large

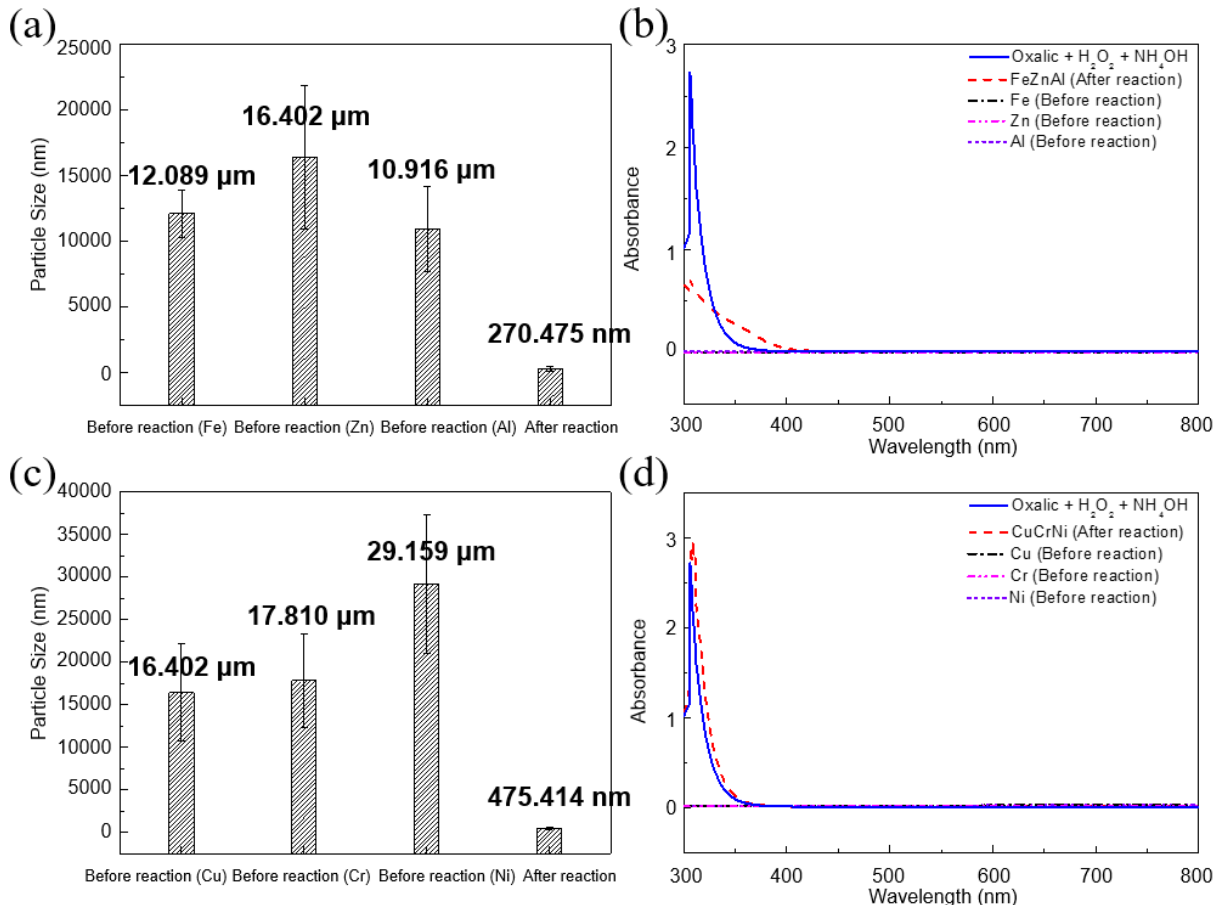


Fig. 2. UV-visible absorption spectra and particle size distribution (a, b) FeZnAl, (c, d) CuCrNi in cleaning solution containing oxalic acid

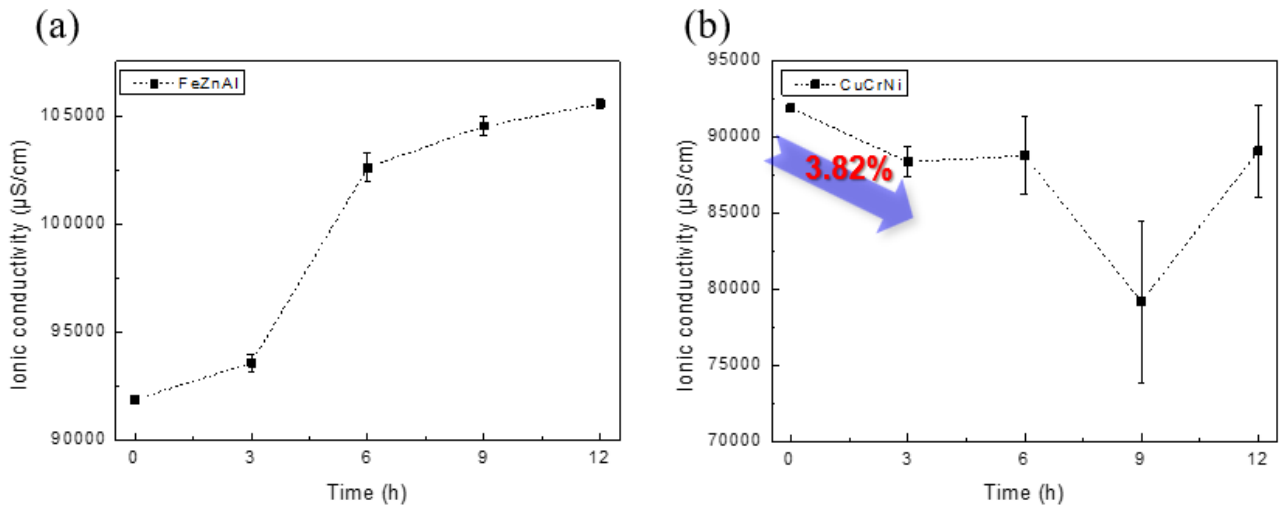


Fig. 3. Ionic conductivity change behavior of (a) FeZnAl and (b) CuCrNi with time

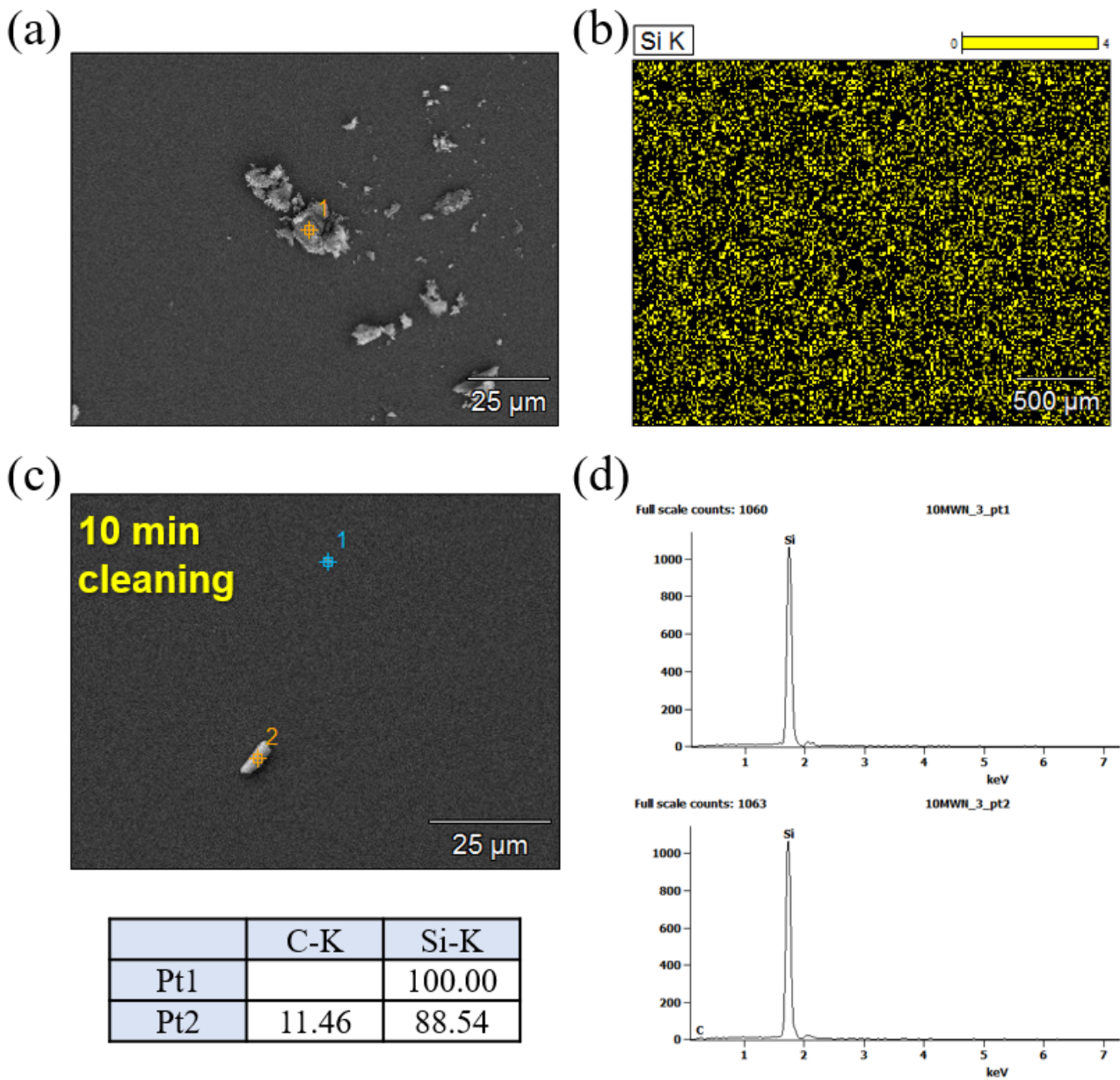


Fig. 4. Analysis of wafer surface shape and elements before and after cleaning (a) waste wafer surface shape, (b) analysis of cleaned wafer surface elements, (c) wafer surface shape after cleaning (d) the cleaned wafer surface particle element analysis

amount of impurities existed on the surface of the waste wafer. As shown in Fig. 4(b), it was confirmed that particles remaining on the cleaned wafer surface were not detected, and secondary phases other than Si were not detected. Therefore, it is expected that the cleaning with oxalic acid was smoothly performed. Fig. 4(c) shows the enlarged wafer surface. As shown in Fig. 4(c), a small amount of residual particles were detected, and as a result of elemental analysis as shown in Fig. 4(d), it was confirmed as Si. Thus, the particles on the surface of the wafer are expected to be Si particles that generated during the sampling process. Therefore, since metal impurities such as Table 1 detected on the wafer surface before cleaning were not detected after cleaning, it is expected that cleaning proceeded smoothly. In addition, since defects such as vacancy did not appear in the shape of the cleaned wafer surface, the effect of the cleaning solution on the wafer is expected to be insignificant.

4. Conclusions

This study attempted to prepare an ideal cleaning solution for cleaning waste wafers. Before the reaction, it was confirmed that all metal powders showed a particle size distribution of 10 μm or more, but a particle size distribution of 500 nm or less after the reaction. In addition, as the result of UV analysis, since the metals before and after the reaction showed different absorbances, it is expected that the metals reacted with the cleaning solution to form coordination compounds. As a result of the ionic conductivity analysis, the ionic conductivity before and after the reaction for 3 hours showed a slight difference, so it is expected that the chelating agent prevented the decomposition of H_2O_2 . In order to confirm the wafer cleaning characteristics of the cleaning solution, the wafer surface shape and elemental analysis were performed before and after cleaning. Unlike waste wafer before cleaning, the wafer after cleaning did not show any additional phases other than Si, and defects such as vacancy were not detected. Through this, the applicability of the cleaning solution to which the chelating agent was added was confirmed.

Acknowledgments

This work was supported by Korea Technology & Information Promotion Agency for SMEs(TIPA) grant funded by the Ministry of SMEs and Startups(MSS) (S2825750).

REFERENCES

- [1] K. Liu, D. Zuo, X.P. Li, M. Rahman, J. Vac. Sci. Technol. B: Microelectronics and Nanometer Structures **27** (3), 1361-1366 (2009).
- [2] M. Kim, K. Ryu, K.J. Lee, J. Korean Powder Metall. Inst. **28** (1), 25-30 (2021)
- [3] W. Kern, J. Electrochem. Soc. **137** (6), 1887-1892 (1990).
- [4] O.J. Anttila, J. Electrochem. Soc. **139** (4), 1180-1185 (1992).
- [5] K. Saga, J. Electrochem. Soc. **143** (10), 3279-3284 (1996).
- [6] M. Itano, F.W. Kern, M. Miyashita, T. Ohmi, IEEE Trans. Semicond. Manuf. **6** (3), 258-267 (1993).
- [7] W. Kern, Handbook of silicon wafer cleaning technology, United States 2018.
- [8] M. Matsuo, T. Takahashi, H. Habuka, A. Goto, Mat. Sci. Semicon. Proc. **110**, 104970 (2020).
- [9] G.W. Gale, D.L. Rath, E.I. Cooper, S. Estes, H.F. Okorn-Schmidt, J. Brigante, R. Jagannathan, G. Settembre, E. Adams, J. Electrochem. Soc. **148** (9), G513-G516 (2001).
- [10] D. Liu, Z. Li, Y. Zhu, Z. Li, R. Kumar, Carbohydr. Polym. **111**, 469-476 (2014).
- [11] J.B. Fein, Geology **19** (10), 1037-1040 (1991).
- [12] N. Zubair, K. Akhtar, Trans. Nonferrous Met. Soc. China **29** (1), 143-156 (2019).
- [13] D. Nansheng, W. Feng, L. Fan, L. Zan, Chemosphere **35** (11), 2697-2706 (1997).
- [14] A.K. Sharma, A. Singh, R.K. Mehta, S. Sharma, S.P. Bansal, K.S. Gupta, Int. J. Chem. Kinet. **43** (7), 379-392 (2011).
- [15] M.Z. Mubarak, J. Lieberto, Procedia Earth Planet. Sci. **6**, 457-464 (2013).
- [16] D. Rai, B.M. Sass, D.A. Moore, Inorg. Chem. **26** (3), 345-349 (1987).
- [17] C.H. Bamford, R.G. Compton, C.F.H. Tipper, Reactions of metallic salts and complexes, and organometallic compounds, Elsevier 1972.